Biochemistry

Article

Cite This: *Biochemistry* 2018, 57, 3966–3975

pubs.acs.org/biochemistry

Peptidoglycan and Teichoic Acid Levels and Alterations in *Staphylococcus aureus* by Cell-Wall and Whole-Cell Nuclear Magnetic Resonance

Joseph A. H. Romaniuk and Lynette Cegelski*

Department of Chemistry, Stanford University, 380 Roth Way, Stanford, California 94305, United States

Supporting Information

ABSTRACT: Gram-positive bacteria surround themselves with a multilayered macromolecular cell wall that is essential to cell survival and serves as a major target for antibiotics. The cell wall of *Staphylococcus aureus* is composed of two major structural components, peptidoglycan (PG) and wall teichoic acid (WTA), together creating a heterogeneous and insoluble matrix that poses a challenge to quantitative compositional analysis. Here, we present ^{13}C cross polarization magic angle spinning solid-state nuclear magnetic resonance (NMR) spectra of intact cell walls, purified PG, and purified WTA. The spectra reveal the clear molecular differences in the two polymers and enable quantification of PG and WTA in isolated cell walls, an attractive alternative to estimating teichoic acid content from a phosphate analysis of completely pyrolyzed cell walls. Furthermore, we discovered that unique PG and WTA spectral signatures could be identified in whole-cell NMR spectra and used to compare PG and WTA levels among intact bacterial cell samples. The distinguishing whole-cell ^{13}C NMR contributions associated with PG include the GlcNAc-MurNAc sugar carbons and glycyl α-carbons. WTA contributes carbons from the phosphoribitol backbone. Distinguishing ^{15}N spectral signatures include glycyl amide nitrogens in PG and the esterified D-alanyl amine nitrogens in WTA. ^{13}C NMR analysis was performed with samples at natural abundance and included 10 whole-cell sample comparisons. Changes consistent with altered PG and WTA content were detected in whole-cell spectra of bacteria harvested at different growth times and in cells treated with tunicamycin. This use of whole-cell NMR provides quantitative parameters of composition in the context of whole-cell activity.

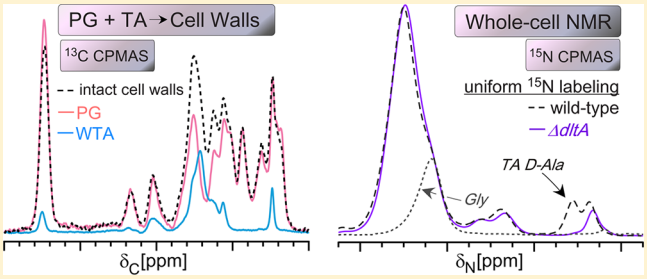

Gram-positive bacteria surround themselves with a thick cell wall that is essential to cell survival and is a major target of antibiotics. The cell wall is composed primarily of two polymeric macromolecules, peptidoglycan (PG) and wall teichoic acids (WTAs), with their chemical structures in *Staphylococcus aureus* provided in Figure 1. Bacterial cell-wall composition, assembly, and function have been intensely investigated over many decades. This rich history is a result of the natural and intense curiosity to understand how such a self-assembly process occurs, coupled with the urgent need for new strategies to prevent and treat infectious diseases.

The inhibition of cell-wall synthesis is a well-pursued avenue for the identification of antibiotics, where most cell-wall targeting antibiotics are thought to inhibit specific steps in PG biosynthesis or inhibit very early steps in cell-wall synthesis central to both PG and WTA.[1] PG assembly is essential to cell viability and provides the strong yet dynamic structural scaffolding that surrounds and mechanically protects cells from their internal turgor pressure. Core enzymatic steps in peptidoglycan synthesis have been carefully elaborated and require the coordinated activity of more than 10 proteins.[2] PG biosynthesis begins in the cytoplasm, ultimately leading to the production of Lipid II, the complete PG subunit (Figure 1) attached to the membrane-associated bactoprenol-pyrophosphate lipid carrier.[3] Lipid II is then translocated to the outside of the cell through the newly appreciated role of a flippase, whose mode of action is of intense interest and under study.[4] At the cell surface, the PG subunit is released from the lipid carrier and added to existing PG through the action of transglycosylation and transpeptidation. Cell-wall-associated proteins can also be covalently linked to the terminus of the glycyl bridge in place of a cell-wall cross-link to another PG subunit. Additional cell-wall biosynthesis proteins remain under study for their potential roles as flippases and as additional transglycosylation and transpeptidation enzymes.[5]

WTAs are covalently attached to PG MurNAc residues, a process that occurs outside the cell.[6] Cell-wall modification with WTA is implicated in virulence and host adherence,[7] decreased antibiotic susceptibility,[8,9] and resistance to cationic antimicrobial peptides and antibodies.[10] Thus, although PG biosynthesis has long been a target for effective antibiotics, targeting WTA biosynthesis is an attractive approach to inhibiting virulence and increasing susceptibility of bacteria to currently available antibiotics.[11,12] In addition, targeting WTA

Received: April 30, 2018
Revised: May 25, 2018
Published: May 28, 2018

DOI: 10.1021/acs.biochem.8b00495
Biochemistry 2018, 57, 3966–3975

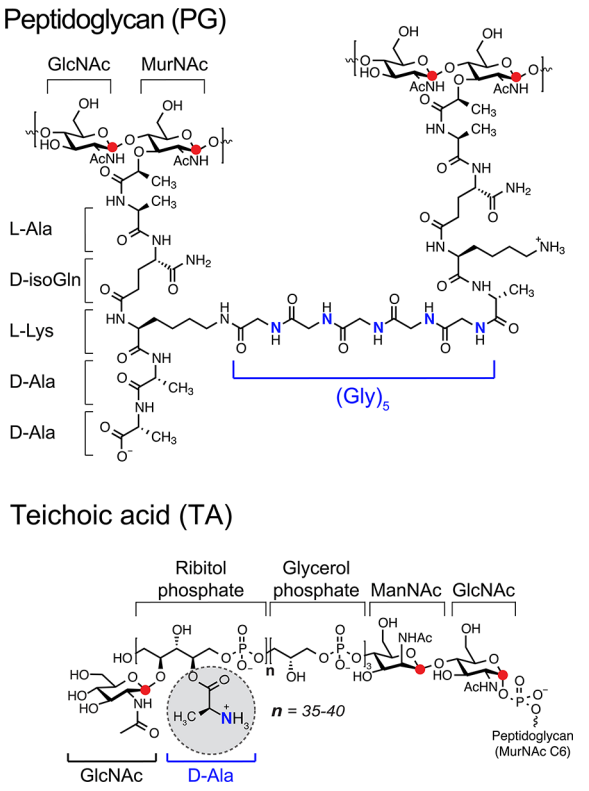

Figure 1. Chemical structures of PG and WTA. (A) In *S. aureus*, peptidoglycan is composed of a repeating unit of the disaccharide *N*-acetylmuramic acid (MurNAc)-(β-1,4)-*N*-acetylglucosamine (GlcNAc) with an attached peptide stem that is cross-linked to a neighboring peptide stem through the pentaglycine bridge of one stem and the penultimate D-Ala of the neighboring stem. Cross-link formation occurs with the loss of the terminal D-Ala. (B) Wall teichoic acids are composed of long chains of polyribitol phosphate (35−40 units) and are covalently anchored to peptidoglycan through a short (1−3 units) polyglycerol phosphate bridge and the disaccharide *N*-acetylmannosamine (ManNAc)-(β1→4)-GlcNAc. The ribitol phosphate units are additionally modified with GlcNAc and D-Ala esters. Anomeric carbons are colored red, and glycine amide nitrogens and the TA D-Ala amine are colored blue.

assembly holds promise to inhibit viability vis-à-vis antibacterial activity.[13] WTA had not traditionally been considered as essential to cell growth because strains that cannot produce WTA and cells treated with inhibitors that affect the very first stages of WTA synthesis are viable, even though they exhibit altered morphology and septation.[12] However, inhibition of later stages of WTA synthesis can be lethal, thus revealing a specific target for antibacterial development.[14]

WTA biosynthesis begins in the cytoplasm to produce the C55-lipid-linked immature WTA polymer, the ManNAc-GlcNAc disaccharide followed by three glycerol phosphates, and then a longer polymer of ribitol phosphate groups (~40 units).[15] Ribitol units can be modified with GlcNAc while still on the cytosolic side of the membrane.[16] Transporter proteins flip the extended WTA polymer to the extracellular surface,[17] where it is linked to PG.[6,18] D-Alanylation of ribitol units is thought to occur extracellularly and is mediated by the DltA, DltB, DltC, and DltD proteins.[19] Lipoteichoic acid (LTA) is also produced by Gram-positive bacteria but is integrally associated with the cell membrane. LTA synthesis follows an independent pathway, with an important distinction of being composed of polyglycerol phosphate groups, not ribitol phosphate as in WTA. In contrast to ribitol in WTA, the glycerol in LTA only has one hydroxyl functional group, and it can be modified with either GlcNAc or D-Ala.[20−22]

Many currently available antibiotics target PG biosynthesis. For example, fosfomycin inhibits MurA and prevents the synthesis of MurNAc in the cytosol.[23] Vancomycin, a glycopeptide antibiotic, sequesters the cell-wall precursor, Lipid II, at the cell surface, prevents incorporation of the subunit into the growing PG strands, and reduces the supply of lipid carrier available for further peptidoglycan synthesis.[24] However, for some antibiotics, ambiguities from available experiments prevent a definitive determination of the molecular basis of action during cell growth. For example, the β-lactams and cephalosporins inhibit PG assembly by inhibiting cross-linking as a substrate mimic and suicide inhibitor of transpeptidation domains of penicillin binding proteins, so named for this activity.[1] However, there has been a recent resurgence in mechanistic studies examining β-lactam antibiotic modes of action in terms of cell killing activity. Work with *Escherichia coli*, for example, demonstrated that the cell killing activity of mecillinam is more complex and includes activation of a futile cycle of cell-wall production and turnover that depletes available PG precursors.[25] A newly identified antibiotic, teixobactin, binds to isolated lipid-linked precursors of both peptidoglycan and teichoic acids *in vitro*, as observed in a thin layer chromatography binding assay,[26] yet teixobactin's precise mechanism or multiple mechanisms operating during growth are uncertain.[27] Lysobactin was also observed to bind both PG and WTA lipid-linked precursors through *in vitro* enzymatic competition assays, although the killing action was more recently suggested to be due to its Lipid II binding activity through observation of an accumulation of Lipid II in lipid extracts of treated cells.[28] Complementary avenues of investigation for examining antibiotic modes of action during cell growth are always desired.[29]

New methods are continually being introduced to probe and evaluate cell-wall assembly *in vivo* to address ambiguities that can result during investigations of antibiotic modes of action, particularly given the challenge of identifying and quantifying chemical and structural changes to the insoluble cell-wall polymers. Classical approaches include the tracking of radiolabeled cell-wall precursors through the steps of synthesis and the analysis of enzymatic and acid digests of cell walls by chromatographic separation and detection [e.g., high-performance liquid chromatography (HPLC) or liquid chromatography and mass spectrometry (LC−MS)].[30] These classic techniques work especially well and can provide quantitative data in Gram-negative bacteria with their completely hydrolyzable PG. In *S. aureus*, however, the PG cannot be completely solubilized; even after extensive digestion by cell-wall hydrolases and acid, an inseparably cross-linked, high-molecular weight polymer remains. This incomplete dissolution prevents a complete accounting of PG components by solution-based methods such as HPLC.[31] Newer methods include strategies for fluorescently labeling peptidoglycan for live-cell imaging.[32] Although fluorescently labeled amino acid analogues can be cytotoxic, at limited concentrations they enable visualization of incorporation of the analogue into the cell wall to characterize, for example, the activity of different penicillin binding proteins and the spatial mapping of cell-wall synthesis sites.[33] Studies to establish the intermediates and products of peptidoglycan synthesis have additionally leveraged creative biochemical

DOI: 10.1021/acs.biochem.8b00495
Biochemistry 2018, 57, 3966−3975

experiments including *in vitro* reconstruction of the enzymatic pathways.[6]

Toward the goal of obtaining parameters of composition and architecture in cell walls and whole cells, we have introduced strategies using solid-state NMR spectroscopy. Quantitative determinations can be made of lysyl coupling to the pentaglycine bridge (bridge-links) and of D-Ala-Gly cross-links through nonperturbative labeling during cell growth using selectively ^{13}C- and ^{15}N-labeled amino acids.[34,35] Whole-cell NMR of *S. aureus* treated with vancomycin suggested that vancomycin sequesters Lipid II, thereby preventing transglycosylation, and does not significantly influence transpeptidation.[34] Internuclear distances have also been measured between antibiotics and cell-wall sites in whole cells,[35] and additional reports have measured parameters of cell-wall architecture.[36−38] In addition, solid-state NMR analysis of intact cell-wall samples provided quantitative ratios of distinct types of PG units that are not possible with HPLC analysis that reports only on the soluble material liberated from attempted digestion of the cell wall.[32] ^{31}P solid-state NMR analyses of teichoic acids have also addressed dynamics of the WTA and the binding of metal cations.[39,40] In addition, mass spectrometry has been employed to detect teichoic acids produced by clinical isolates.[41]

As debate continues over how some antibiotics, like the β-lactams, function to cause cell death in bacteria,[25] solid-state NMR offers a means to extract chemical and structural information about cell-wall composition and antibiotic action. We present here a new strategy, demonstrating that interpretable and quantifiable spectral changes in cell-wall and whole-cell samples can report on changes to PG and WTA without any selective labeling. Samples are examined either at natural abundance ^{13}C or through previously reported uniform labeling in which all carbons are labeled with ^{13}C or all nitrogens are labeled with ^{15}N in the cell-wall and whole-cell samples.[42,43] We present an extensive comparative sample analysis, including 10 whole-cell NMR samples and cells treated with a teichoic acid inhibitor (tunicamycin), to emphasize the sensitivity of the whole-cell NMR approach.

MATERIALS AND METHODS

Bacterial Cultures and Whole-Cell NMR Sample Preparation. *S. aureus* strains were routinely maintained on tryptic soy agar (TSA) plates or in tryptic soy broth (TSB). Uniformly labeled *S. aureus* (strain MW2 and mutants MW2Δ*tarO* and MW2Δ*dltA*) were prepared from growth in a modified version of *S. aureus* synthetic medium (SASM). As previously described, the modified SASM contained a uniformly labeled ^{13}C and ^{15}N algal amino acid extract instead of the individual 20 amino acids and had glucose and ammonium sulfate replaced with their uniformly labeled ^{13}C and ^{15}N counterparts, respectively.[42] Bacteria prepared with selective labels, either L-[ε-^{15}N]lysine or [^{15}N]glycine, were grown in standard SASM in which the indicated amino acid was replaced with its labeled counterpart. For D-[^{15}N]alanine labeling, 100 mg/L D-[^{15}N]alanine was added to regular SASM, and the cultures were grown with 10 μg/mL alaphosphin, an alanine racemase inhibitor, to prevent scrambling of D-Ala and L-Ala.[35] All bacterial cultures were grown to an optical density (OD) at 600 nm of 1.0 (or an otherwise specified OD) at 37 °C with 200 rpm shaking and harvested by three cycles of centrifugation at 10000*g* and washing with 5 mM, pH 7.0 HEPES buffer. Final cell pellets were frozen with liquid nitrogen and lyophilized. Lyophilized sample pellets were used for solid-state NMR analysis. Most whole-cell samples were harvested from 300 mL of culture and yielded a cell pellet with a dry mass between 50 and 100 mg.

Isolated Cell-Wall, PG, and WTA Sample Preparation. *S. aureus* MW2 cultures for cell-wall, PG, and WTA isolations were grown as described above to an OD of 4.0 in tryptic soy broth (no labels). Cell walls were isolated through an established protocol.[31] Isolated PG was extracted following the same protocol but used mutant *S. aureus* cells lacking the *tarO* gene necessary for WTA synthesis (MW2Δ*tarO*). Teichoic acids were liberated from wild-type (MW2) purified cell walls. This liberation involved treating purified cell walls with 30 mL of 0.1 M sodium hydroxide for 18 h at 37 °C and 200 rpm shaking, followed by neutralization with 30 mL of 0.1 M acetic acid. Centrifugation at 38000*g* for 1 h removed nonhydrolyzed cell-wall components, and the supernatant containing WTA was collected, dialyzed extensively against water in a 3.5 kDa molecular weight cutoff dialysis membrane, and then flash-frozen and lyophilized for NMR studies.

Solid-State NMR Spectroscopy. Solid-state NMR experiments were performed using an 89 mm 11.7 T wide-bore magnet (500.92 MHz for ^{1}H, 125.96 MHz for ^{13}C, and 50.76 MHz for ^{15}N), a Varian console with VNMRJ software, a home-built four-frequency transmission-line probe with a 13.6 mm long, 6 mm inner diameter sample coil, and a Revolution NMR magic angle spinning Vespel stator. American Microwave Technology RF power pulse amplifiers (M3445B, 2 kW, Herley Inc.) were used to produce radiofrequency pulses for ^{15}N (50 MHz) and ^{13}C (125 MHz), while the ^{1}H (499 MHz) radiofrequency pulses were generated with a 2 kW tube amplifier (Amplifier System Inc., Herley Inc.) driven by a 50 W American Microwave Technology power amplifier (M3900C-2, Herley Inc.) under active control.[44]

Samples were spun at 7143 ± 2 Hz in thin-wall 5 mm outer diameter zirconia rotors. The temperature was maintained at ∼5 °C, controlled by a variable-temperature stack (FTS Systems Inc.). ^{13}C or ^{15}N cross polarization magic angle spinning (CPMAS)[45] spectra were obtained with a contact time of 1.5 ms, with spin−echo detection, and a recycle delay of 2.0 s. Field strengths for ^{13}C and ^{15}N cross-polarization were all 50 kHz with π-pulses of 10 μs and with a 10% linear ^{1}H ramp centered at 57 kHz. ^{1}H decoupling was performed at 72 kHz (continuous wave) during acquisition. The CPMAS mixing time was 1.5 ms and the recycle time 2.0 s for all experiments. The CP mixing time was incremented between 0.5 and 8 ms for CP array experiments. ^{13}C chemical shifts were referenced to tetramethylsilane as 0.0 ppm using a solid adamantine sample at 38.5 ppm. The ^{15}N chemical shift scale is referenced to ammonia as 0 ppm.

NMR Spectral Analysis. For estimating PG and WTA carbon contributions to whole cells, ^{13}C CPMAS spectra of PG and WTA were added until the summed spectrum best recapitulated the full cell-wall spectral intensity, noting the expected intensity match between the glycyl α-carbon peak in the cell-wall and PG spectra, wherein WTA does not contain glycine. The integrated areas of the PG and WTA spectra were then used to calculate the percent of each component contributing to the cell-wall spectrum to estimate the relative ratio of total PG versus WTA carbons. The carbon percentage was converted to an overall mass percentage using the average chemical formulas for PG ($C_{46}H_{82}N_{14}O_{22}$, 1206 g mol^{-1}) and WTA ($C_{544}H_{1084}N_{42}O_{608}P_{44}$, 18199 g mol^{-1}) units. These are

DOI: 10.1021/acs.biochem.8b00495
Biochemistry 2018, 57, 3966−3975

the respective formulas for a pentaglycine-muropeptide PG unit, and an intact chain of WTA that is fully modified with *N*-acetylglucosamine and bearing 40 repeat units of ribitol phosphate.

Quantification of peak areas in the whole-cell spectra was performed as follows. For whole-cell ^{13}C CPMAS spectra, the anomeric carbon peak area at 101 ppm in each spectrum was well resolved and calculated using a Gaussian peak fit to the anomeric carbon peak using Matlab and provided in Figure S2. The calculated area was divided by the total spectral area to provide a quantitative parameter of anomeric carbon contributions to each spectrum. The same protocol was used for the D-Ala amine nitrogen at 38 ppm in each uniformly labeled ^{15}N whole-cell CPMAS spectrum. A specifically labeled [^{15}N]Gly whole-cell spectrum was available, and this enabled the experimental glycyl amide peak to be used directly for fitting and estimating the glycyl amide nitrogen contribution to each ^{15}N spectrum, centered at 108 ppm. A simple integral of the total amide area (including the glycine) was also measured. Spectral plotting and fitting were performed using Matlab and Igor Pro software.

Inorganic Phosphate Determination. The inorganic phosphate content of cell walls, PG, and WTA was assayed through the method of Chen et al., as modified by Ames and Dubin.[46,47] Briefly, isolated samples were resuspended in deionized water to approximately 1 mg/mL. Twenty microliters of sample was mixed with 50 μL of 10% magnesium nitrate in ethanol. Samples were heated to dryness in a Bunsen burner and ashed until no brown fumes evolved and a white powder remained. The powder was dissolved in 300 μL of 1 M hydrochloric acid and incubated for 1 h. The samples were then mixed with 700 μL of a mixture of one part 6 N hydrochloric acid, one part 2.5% ammonium molybdate in water, two parts deionized water, and one part freshly prepared 10% ascorbic acid in water. The mixtures were incubated at 45 °C for 30 min, and then the absorbance at 820 nm was read. The absorbance of each sample was compared to those of phosphoric acid standards treated in the same manner to calculate the phosphate content.

RESULTS

^{13}C CPMAS Spectra of Purified Peptidoglycan and Wall Teichoic Acid. Solid-state NMR spectroscopy was employed to define and quantify the spectral contributions of PG and TA to *S. aureus* cell walls *in situ*. As revealed in previous work, a high-quality preparation of isolated cell walls yields a ^{13}C CPMAS spectrum with well-defined peaks consistent with the carbon contributions expected for PG and WTA (i.e., anomeric carbons, ring sugar carbons, ribitol carbons, and carbonyl and methyl carbons associated with glycan acetylation) as well as PG peptides, including the uniquely resolved glycine α-carbon peak at 42 ppm (Figure 2A).[42] Here, for the first time, we present the ^{13}C NMR spectra for separate samples of purified PG and purified WTA. Purified PG was isolated from a *S. aureus* mutant unable to synthesize teichoic acid, MW2Δ*tarO*.[48] Purified WTA was isolated through a procedure beginning with purified cell walls from wild-type cells. After isolation of intact cell walls, WTA was liberated into the solution through alkaline hydrolysis and separated from PG through centrifugation. The only amino acid contributions to the isolated cell-wall spectrum should originate from PG. WTA is D-alanylated in whole cells, but the esterified D-Ala is eliminated through hydrolysis during cell-wall isolations. Thus,

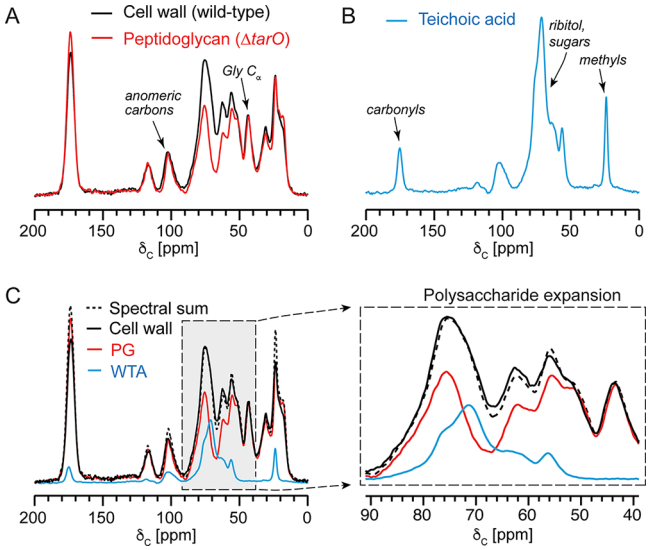

Figure 2. ^{13}C CPMAS spectra of isolated PG and WTA and spectral contributions to isolated cell walls. (A) Natural abundance ^{13}C CPMAS spectra of cell walls isolated from *S. aureus* MW2 (black) and MW2Δ*tarO* (red). The cell walls from MW2Δ*tarO* represent only peptidoglycan. (B) Natural abundance ^{13}C CPMAS spectrum of WTA isolated from MW2 cells. (C) Scaled spectral sum (black dashed line) of the WTA and PG spectra presented as an overlay with the three individual sample spectra. The PG and WTA spectra were scaled such that the spectral sum matched the full intensity of the glycyl α-carbon and the polysaccharide region. All spectra were acquired with 32768 scans, and sample sizes were 80 mg for cell walls, 20 mg for PG, and 40 mg for WTA.

a straightforward way to compare the contribution of the PG ^{13}C spectrum to that of the intact cell walls is to normalize the two spectra by the glycine α-carbon peak, given that glycine in the cell wall arises from only PG and not at all from WTA. This comparison of the PG ^{13}C NMR spectrum with the cell-wall spectrum first suggested that PG is the dominant contributor by carbon mass to the cell wall (Figure 2A). Second, the major spectral difference between these two was for carbon intensities unique to the isolated WTA ^{13}C CPMAS spectrum, which is dominated by the ribitol carbons just upfield of the 78 ppm PG sugar region (Figure 2B). In addition, the WTA spectrum reports on the approximately one GlcNAc modification per ribitol unit, with acetyl group carbonyl and methyl carbon chemical shifts at 175 and 22 ppm, respectively. D-Alanyl esters decorate WTA in the context of cells but are hydrolyzed and removed during the cell-wall isolation and, thus, not present in isolated WTA. Thus, we identified differentiating PG and TA carbon contributions to the one-dimensional ^{13}C spectrum of isolated cell walls that will be of value in comparing PG and TA content among different intact cell-wall preparations.

Teichoic Acid and Peptidoglycan Contributions to Cell Walls. We sought to determine whether a spectral sum of the ^{13}C spectra of the purified cell-wall parts (PG and WTA) would recapitulate the ^{13}C spectral intensity in the intact cell-wall sample. This would enable a new approach to estimating PG and WTA content in isolated cell walls. If successful, the unique PG and WTA spectral signatures should also be able to report on PG and WTA content in unperturbed whole-cell samples given the high percentage of cell wall by mass in whole cells.

DOI: 10.1021/acs.biochem.8b00495
Biochemistry 2018, 57, 3966−3975

Indeed, a spectral sum of the PG and WTA spectra recapitulated the spectrum of intact cell walls quite well in most peaks, with small differences in the peaks associated with acetylation (Figure 2C). The difference in acetylation is likely attributed to altered PG acetylation when PG is produced in the context of the *tarO* mutant, where PG would exhibit an increased level of O-acetylation in the absence of TA or where the O-acetyl groups in MW2Δ*tarO* are more stable because of the cell-wall isolation protocol. Interestingly, O-acetylation of MurNAc in *S. aureus* is associated with resistance to lysozyme, and acetylation can be influenced in different conditions.[49,50] Nevertheless, to estimate the ratio of PG and WTA from the cell-wall spectrum, the primary polysaccharide region of the spectrum and PG and WTA spectra were examined. A simple addition of the PG and WTA spectra in Figure 2 resulted in the close match to the polysaccharide region of the isolated cell-wall spectrum and satisfied the expectation that the glycyl α-carbon peak intensity in the cell-wall spectrum arises entirely from the PG spectrum, because WTA does not contain glycine. Through peak integration and conversion of the integrated carbon spectral area as a proxy for carbon mass percent to overall molecular mass percent, together with the average WTA chemical formula, we determined that TA accounts for 22% of the cell wall by mass and PG makes up the remaining 78% in cells harvested at an OD of 4.0.

Teichoic acid levels are typically estimated by fully digesting cell-wall material and quantifying phosphate released from fully pyrolyzed cell-wall samples.[39,51] Using phosphate analyses, estimates of teichoic acid by mass are then made by calculating the expected mass of the complete WTA unit associated with each WTA chain, assuming one phosphate per ribitol phosphate and three glycerol phosphate units as shown in Figure 1. The NMR estimate was within error of the estimate of that from our phosphate analysis (Figure S1), wherein the molecular formula for WTA in the isolated cell wall (as in Figure 1) is $C_{544}H_{1084}N_{42}O_{508}P_{44}$. This value is also consistent with some previous reports of WTA content in *S. aureus*, yet using ^{13}C CPMAS NMR, one can immediately evaluate the composition of the entire cell-wall preparation and observe any obvious alterations in chemical composition, such as altered acetylation, which could be indicative of modifications to PG and/or WTA. We next sought to extend the NMR approach to monitoring PG and WTA in intact cells.

Specific PG and TA Carbon Signatures Report on Composition in Intact Bacterial Cells. The cell wall of *S. aureus* accounts for 15−25% of the mass of the cell wall, depending on the stage of growth and cell-wall thickness.[31] Given the distinctive composition of the cell wall compared to those of other cellular components, cell-wall-specific NMR peaks can be detected within a whole-cell NMR spectrum, even without selective isotopic labeling. Most of the anomeric carbon peak intensity at 100 ppm, for example, is attributed generally to the bacterial cell wall as confirmed by comparison with protoplast preparations and cells treated with cell-wall inhibiting antibiotics.[42] We tested the ability of a whole-cell NMR approach to differentially detect and compare the relative contributions of WTA versus PG in whole-cell samples without the need for cell-wall isolations.

We compared ^{13}C CPMAS spectra of wild-type *S. aureus* and *tarO* mutant cells, lacking WTA (Figure 3). Compared to the whole-cell ^{13}C spectrum of wild-type cells, that of the *tarO* mutant exhibited a reduction in the polysaccharide region (60−90 ppm). The reduction is most prominent near 69 ppm, the ribitol region identified in the isolated WTA sample described above (Figure 3). LTA glycerol carbons would generally contribute to this spectral region but should peak near 74 ppm. The anomeric carbon peak intensity is slightly greater for the *tarO* mutant, possibly indicative of more PG, which would parallel observations of aberrant cell-wall division and accumulated cell wall in MW2Δ*tarO*.[12] This will be supported below by ^{15}N measurements. Thus, we use the anomeric and ribitol carbon peaks to first monitor and attempt to gauge PG and WTA compositional status, respectively, in intact cells.

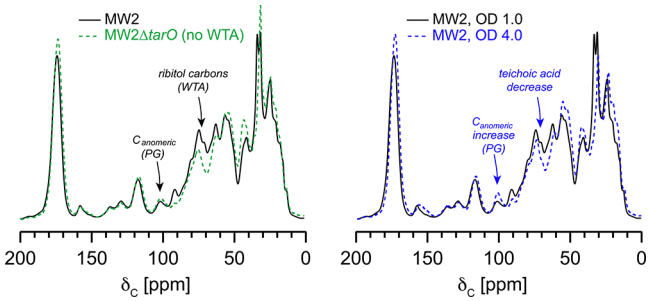

Figure 3. ^{13}C CPMAS spectra of intact *S. aureus* cells. ^{13}C CPMAS spectra of wild-type (black) and *tarO* mutant (green) whole cells, both harvested at an OD_{600} of 1.0 (left). ^{13}C CPMAS spectra of whole cells at OD_{600} values of 1.0 and 4.0 (right). Spectra were acquired with 32768 scans.

Using these ^{13}C spectral signatures, we made a new observation regarding the balance of PG and WTA as a function of growth state. For cells harvested during the exponential phase (OD values of 0.5 and 1.0), the intensity of the anomeric carbon was similar in height and area to those of aromatic carbons associated with rRNA and aromatic amino acid residues at 129 and 158 ppm.[52] For cells harvested from the stationary phase (OD values of 2.0 and 4.0), the anomeric peak intensity increased (Figure 3 and Figure S3). This observation is consistent with our previous transmission electron microscopy analysis, showing cell-wall thickening, and NMR measurements in isolated cell walls using specific isotopic lysine labeling.[31] However, an opposite trend was observed for the ribitol peaks: as cells reached the stationary phase, the spectral area associated with teichoic acid decreased relative to that of the anomeric carbons. Thus, ^{13}C NMR analysis suggested that cells harvested at an OD of 4 have cell walls with a PG:WTA ratio higher than that of cells harvested at an OD of 1.

The anomeric carbon peak in each spectrum is shift resolved from other carbon types. Thus, the relative area of the anomeric peak can be compared across spectra to quantify the spectral differences. This is not intended to serve as an absolute determination of PG-specific anomeric carbons but as a way to quantify the observed spectral features across many samples. One can compare relative peak areas in different ways, depending on other possible hallmark features of interest, and presenting the relative spectral area compared to the total integrated area is one of the most straightforward ways to compare individual spectral contributions across samples. These comparisons for all the samples are tabulated at the bottom of Figure 4, with full spectra in Figure S3, together with the ^{15}N analyses as described next.

PG and WTA ^{15}N Signatures in Whole-Cell Spectra. In the whole-cell NMR approach, the ^{13}C signatures described above are not used in isolation and are incorporated and framed

DOI: 10.1021/acs.biochem.8b00495
Biochemistry 2018, 57, 3966−3975

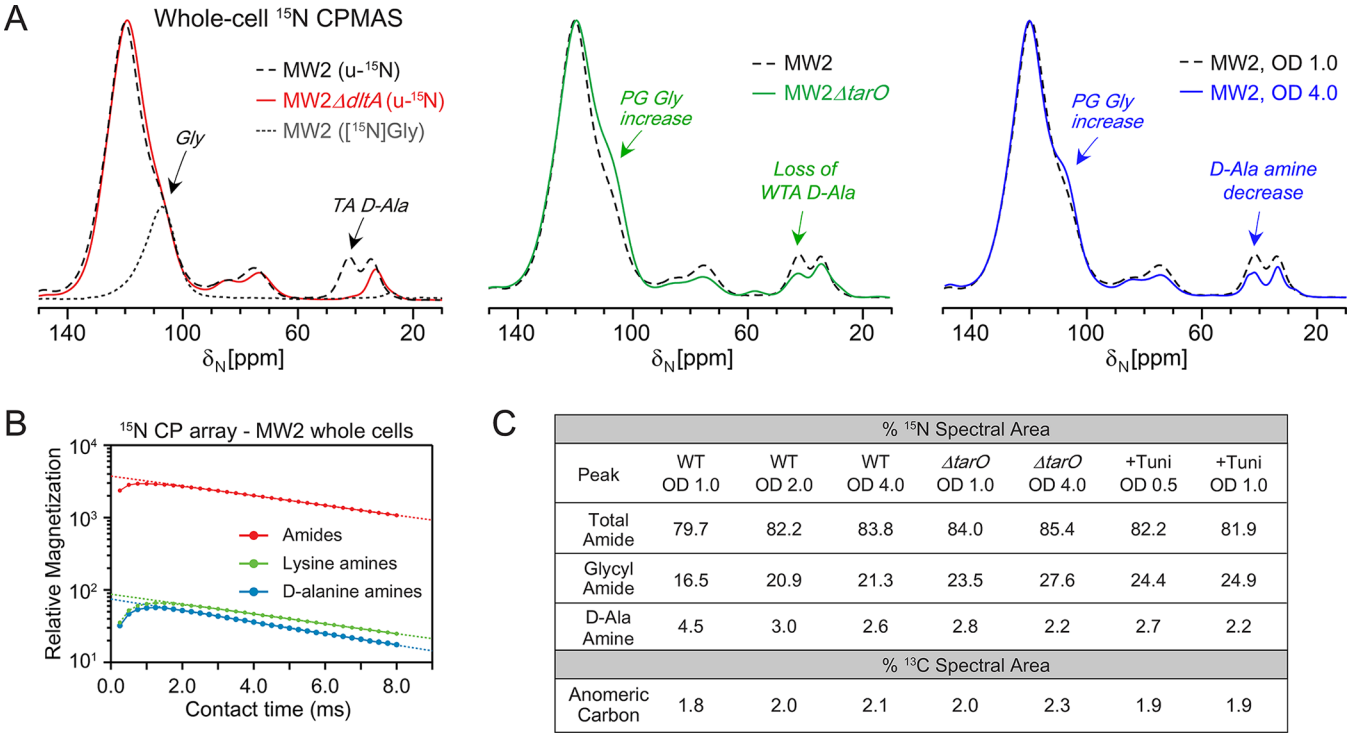

C

% ¹⁵N Spectral Area							
Peak	WT OD 1.0	WT OD 2.0	WT OD 4.0	*ΔtarO* OD 1.0	*ΔtarO* OD 4.0	+Tuni OD 0.5	+Tuni OD 1.0
Total Amide	79.7	82.2	83.8	84.0	85.4	82.2	81.9
Glycyl Amide	16.5	20.9	21.3	23.5	27.6	24.4	24.9
D-Ala Amine	4.5	3.0	2.6	2.8	2.2	2.7	2.2
% ¹³C Spectral Area							
Anomeric Carbon	1.8	2.0	2.1	2.0	2.3	1.9	1.9

Figure 4. ¹⁵N CPMAS spectra of *S. aureus* whole cells. (A) ¹⁵N CPMAS spectral comparisons of MW2 (black) with MW2Δ*dltA* (red) and MW2 Δ*tarO* whole cells, all harvested at an OD of 1.0, and MW2 cells harvested at an OD of 4.0 (blue). A sample labeled selectively with only [¹⁵N]glycine (dashed gray) shows the specific chemical shift contributions of the glycyl amides, abundant in the cell wall (left panel). All spectra are scaled to the amide peak and were acquired with 32768 scans. (B) CP array experiments were performed to examine the $^{1}H-^{15}N$ CP buildup and decay, yielding similar slopes for lines extrapolated from the long contact times for amide and D-Ala amine nitrogens. (C) Percent nitrogen spectral areas for total amides, glycyl amides, and D-Ala amines. The percent carbon spectral area is listed for the resolved anomeric carbon peak in each spectrum.

together with evaluation of ¹⁵N spectra obtained from uniformly ¹⁵N-labeled cells in which all nitrogens in cells are labeled. The nitrogen pools of whole cells are mostly attributed to proteins and nucleic acids (Figure 4). The combined amides (100−120 ppm) dominate the spectrum. Other peaks are ascribed to nucleic acids and protein side chains (70−90 ppm), and amines from components including lysine residues (34 ppm). The peak at 42 ppm has been characterized as having contributions from the D-Ala of teichoic acids.[43] We confirmed this assignment and demonstrated here that the 42 ppm peak is entirely due to teichoic acid D-Ala by comparison with the whole-cell NMR spectrum of a *dltA* mutant, which lacks the *dltA* gene responsible for the D-alanylation of both wall and lipoteichoic acids.[53] In the *dltA* mutant, the 42 ppm signal was abolished (Figure 4). We examined this peak intensity in the *tarO* mutant, which cannot synthesize any WTA but can still synthesize D-alanylated LTA. The D-Ala amine peak intensity decreased compared with that of wild-type cells, wherein the remaining peak intensity in MW2Δ*tarO* is ascribed specifically to LTA D-alanylation. Additional characterization of amine peak contributions was performed using cells labeled selectively with either D-[¹⁵N]Ala or L-[ε-¹⁵N]Lys and confirmed the distinct chemical shifts for alanyl and lysyl amines in whole cells (Figure S4). Previous work with selective lysine labeling and CPMAS and REDOR detection, with CPMAS results recapitulated here in Figure S3, documented the specificity of lysyl amine labeling (with no scrambling in SASM nutrient medium) and established that the efficiency of labeling of lysine is approximately 95% with only 5% dilution by endogenous lysine production.[34] D-Ala and L-Ala selective labeling have also been extensively employed and characterized.[54]

Inspection of ¹⁵N CPMAS spectra of cells harvested during exponential versus stationary phase revealed a decrease in the D-Ala amine nitrogen peak intensity to accompany the reduced ¹³C peak intensity in the ribitol-associated carbon region in Figure 3, together indicative of an overall reduction in the percent of teichoic acid in the sample. Moreover, in MW2Δ*tarO*, the observed D-Ala amine peak can be due to only LTA, because it lacks WTA, and the relative intensity of this D-Ala amine peak decreased for cells harvested in the stationary phase at an OD of 4.0. Thus, the level of LTA D-alanylation was reduced in the MW2Δ*tarO* cells harvested at an OD of 4.0 with respect to PG content. Together with the reduction in the sugar carbons in the corresponding ¹³C whole-cell spectrum for the OD = 4.0 MW2Δ*tarO* cells, this suggests that LTA levels are reduced. If no reduction were observed in the ¹³C spectrum, then such a result would point specifically to a reduction just in the level of D-alanylation of teichoic acids rather than a decrease in total production. Thus, we distinguish between PG- and WTA-specific cell-wall assembly alterations.

Changes in the ¹⁵N glycyl amide region also revealed compositional changes in PG that support the ¹³C NMR observations. The glycyl amide resonance is shifted upfield from other amide resonances and centered at 106 ppm (Figure 4). We demonstrated this specific assignment and unique contribution in whole cells previously using frequency-selective REDOR, identifying these nitrogens as coupled to glycyl α-carbons.[42] We include here an independent way to highlight

DOI: 10.1021/acs.biochem.8b00495
Biochemistry 2018, 57, 3966−3975

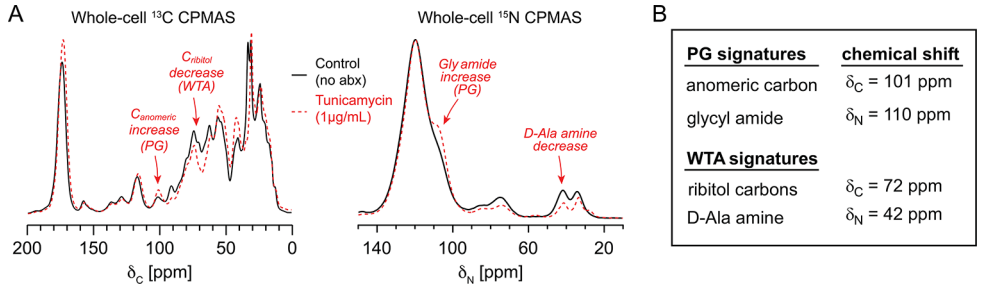

Figure 5. Whole-cell NMR spectra of tunicamycin-treated *S. aureus*. (A) The ^{13}C CPMAS spectrum of cells treated with 1 μg/mL tunicamycin revealed the reduced intensity where ribitol phosphate carbons contribute and an increase in the anomeric carbon peak, ascribed primarily to PG. The ^{15}N CPMAS spectrum of the same tunicamycin-treated sample exhibits an increased glycyl amide shoulder, supporting a relative increase in PG. The decrease in D-Ala amine nitrogen is consistent with a decrease in WTA. (B) ^{13}C and ^{15}N spectral signatures have resulted from examining intact cell walls and purified PG and WTA as well as the whole-cell NMR spectra comparing the influence of growth state and tunicamycin treatment.

this assignment, providing a spectral overlay of whole cells grown in specific [^{15}N]Gly-labeled medium.

The area of the glycyl amide ^{15}N shoulder increased for cells harvested in the stationary phase at OD values of 2 and 4, consistent with an increase in PG production and cell-wall thickening as suggested by the increase in the intensity of the anomeric ^{13}C carbon peak in Figure 3. Thus, the combined carbon and nitrogen NMR spectra provide orthogonal measurements to identify an increase in peptidoglycan and a concomitant decrease in teichoic acid as bacteria slow metabolically and enter the stationary phase. We also examined the ^{15}N spectral area quantitatively to compare relative contributions from the distinct chemical shift regions present in the ^{15}N spectrum to enable more facile comparisons among many samples. We obtained spectra as a function of CP time to generate CP buildup and decay curves for individual peaks to permit absolute quantitative intensity comparisons of the broad amide nitrogen peak and the D-Ala amine peaks, wherein the quantitative intensity is calculated from the *y*-intercept (corresponding to zero contact time) of a line fit to the decay curve to extract the maximum magnetization through CP transfer without relaxation.[55] A total of 32 spectra were obtained, and the ^{15}N peaks exhibited highly similar CP buildup and decay curves (Figure 4 and Figure S5). This is not required for quantification but is an observation that suggests the overall collection of the ^{1}H spins behaves as a homogeneous spin system available for ^{1}H−^{15}N CP. The quantitative peak area percentages (percentage of each peak of the total integrated spectral area) are tabulated in Figure 4C. The glycyl amide shoulder intensity was extrapolated by fitting the region directly with the spectrum of [^{15}N]Gly-labeled cells (Figure S2), noting that the PG pentaglycyl bridge makes a major contribution to this region as evidenced by the major diminution in intensity in protoplast preparations[42] (also included in Figure 4C). These spectral parameters provide a way to quantitatively compare spectral intensities and differences among many samples and NMR spectra. Other specific peak ratios can be obtained and could be valuable for comparing changes between two very specific nuclei in a sample. The ^{15}N CPMAS changes were consistent with the ^{13}C observations reported above. Specifically, the MW2 cells harvested in the stationary phase at an OD of 4.0 exhibit increased amide nitrogen intensity, specifically glycyl amide, consistent with increased PG production and consistent with the increase in the anomeric carbon intensity in the ^{13}C spectrum in Figure 3. The MW2 cells harvested at an OD of 4.0 also exhibit decreased D-Ala amine intensity, indicating reduced TA production per whole-cell sample, which is consistent with the intensity reduction associated with ribitol carbons in Figure 3.

These changes are similar to those observed when comparing wild-type MW2 and MW2Δ*tarO* cells that contain peptidoglycan and LTA but lack WTA. In addition, MW2Δ*tarO* cells harvested at an OD of 4.0, as compared to an OD of 1.0, resulted in an amide (PG) increase and TA (amine) decrease. Thus, the PG-to-LTA mass ratio is greater for cells grown to an OD of 4.0, also consistent with increased PG production in stationary phase cells. CP array data for the uniformly ^{15}N-labeled MW2Δ*tarO* cells are additionally provided in Figure S4D. Thus, a full NMR spectrum reflects the balance of all carbons in the cell, and we have identified salient signatures that can be used to evaluate cell-wall and cellular changes across samples.

Influence of Tunicamycin by Whole-Cell NMR. Through the experiments described above, we demonstrated the ability to evaluate PG and WTA content in whole cells. The anomeric carbon and the glycyl amide nitrogens report on PG levels in whole cells, while the ribitol carbons and D-Ala amines report on teichoic acid levels (WTA and LTA). We used these four signatures to examine the influence of tunicamycin by whole-cell ^{13}C and ^{15}N NMR (Figure 5). Tunicamycin is a compound known to inhibit teichoic acid synthesis and was also reported to influence enzymatic production of PG through *in vitro* enzymatic assays.[13,56] We prepared our samples using a dose of compound of 1 μg/mL, similar to concentrations used to inhibit teichoic acid synthesis,[53] and introduced tunicamycin at the time of inoculation. ^{15}N CPMAS results with tunicamycin-treated cells were comparable to the changes seen in the MW2Δ*tarO* cells (decreased D-Ala amine and increased glycyl amide shoulder). As noted above, a D-Ala amine decrease could simply be due to a decreased level of D-alanylation of WTA or of LTA, and overall conclusions must include consideration of the ^{13}C whole-cell spectra. As observed in the ^{13}C spectrum, tunicamycin resulted in a reduction of peak intensities associated with ribitol carbons (Figure 5A). This is consistent with inhibition of WTA. At the same time, the anomeric carbon and glycyl amide nitrogen levels associated with peptidoglycan increased relative to the control (Figure 5A). These effects were observed for cells harvested at OD values of both 0.5 and 1.0 after treatment with tunicamycin (Figure S4C), conditions that are similar to those used in previous studies.[13,53,56] An increase in peptidoglycan is consistent with aberrant and uncontrolled cell-wall division when teichoic acid synthesis is inhibited, similar to that observed in the *tarO* mutant.[12]

DOI: 10.1021/acs.biochem.8b00495
Biochemistry 2018, 57, 3966−3975

DISCUSSION

Solid-state NMR efforts to characterize bacterial cell walls and the modes of action of antibiotics have been uniquely valuable in dissecting the atomic and molecular details of antibiotics such as oritavancin and analogues, whose modes of action were not clear from biochemical experiments alone.[35,57] Through a comparison of isolated cell walls and purified PG and WTA, we have developed an NMR approach to specifically identify and compare PG and WTA content in isolated cell walls and in intact whole cells. In the former case of isolated cell walls, we can estimate the PG:WTA ratio using the ^{13}C CPMAS spectrum of the isolated cell walls.

As a complex, heterogeneous, and insoluble polymer, there is no other method that provides this PG:WTA estimation in intact, undigested cell walls. Furthermore, the most facile analysis of teichoic acid for quantitative purposes is performed through hydrolysis and phosphate quantification but does not itself provide any other information about composition. An extensive protocol of chemical digestions and LC−MS could be used to analyze composition but is time-consuming and subject to the inability to completely digest PG. We work to address challenges in understanding antibiotic modes of action, for example, where intact cell-wall and whole-cell NMR analyses are needed in mode-of-action determinations and resolving ambiguities from biochemical data. Some strategies have employed selective isotopic labeling strategies, often using pairs of individually labeled amino acids.[31,35,37] However, recently, we have focused on developing approaches that could identify specific compositional information in unlabeled samples with natural abundance ^{13}C NMR analysis or uniform (nonselective) labeling of samples for ^{15}N NMR examinations. Natural abundance ^{13}C NMR approaches are attractive as bacteria could be grown in a complex medium or could be analyzed after being removed from a host setting or an other complex environment.

Moreover, teichoic acids are difficult molecules to study in the context of whole cells. Their abundance can be estimated through indirect measurements of the phosphate content of cell walls,[47] crude measurements of dry weight,[8] or quantification of GlcNAc incorporation with radiometry or D-alanylation through colorimetric assays,[16] yet in all cases, cellular digestions that could be incomplete or associated with cellular debris are required. Solid-state NMR allows for the determination of the composition of the cell walls through direct observation of the combined sum of the carbon chemical shifts present in a cell-wall sample, providing additional inspection of the sample's entire chemical composition and other potential compositional changes. The fitting of the two individual PG and WTA spectra to the cell-wall spectrum yields the quantitative estimate for the PG:TA carbon mass ratio. Doing so, we estimated that ∼22% of the carbon mass of cell walls is due to wall teichoic acids for these cells, noting that the three samples (cell walls, PG, and WTA) were isolated from cells harvested at an OD of 4.0 from growth in TSB nutrient medium. We also observed enhanced acetylation for the purified PG isolated from cells that cannot produce TA. This analysis can be performed on isolated cell walls from samples harvested from different growth states or as a function of growth variables, such as the introduction of inhibitors, to quantify the PG:WTA carbon mass ratio in the cell wall. Importantly, whole-cell spectral changes additionally corroborated observations made from isolated cell walls and can be used to compare large sample sets with the ease of just whole-cell centrifugation and lyophilization for sample preparation, followed by ^{13}C and, ideally, ^{15}N CPMAS analysis. More detailed analysis for important sample comparisons would then be performed on isolated cell-wall samples.

Finally, determining whether a compound interferes with PG and/or teichoic acid synthesis is complicated using biochemical analyses alone. Here, we have presented a holistic, solid-state NMR approach for examining intact *S. aureus* cells to infer whether PG and/or WTA levels are reduced as cell-wall synthesis is inhibited. These analyses would accompany more specific cell-wall NMR studies and could be coupled to specific enzymatic analyses or digestion experiments or additional NMR experiments using selective labeling that quantify specific bond densities, e.g., cross-links. A unique power of solid-state NMR is the ability to quantify chemical composition, to account for the combinations of all carbon types or nitrogen types in samples as complex as whole cells, and also to measure distances and map structures. As shown with the comparison of treatment with the inhibitor tunicamycin, whole-cell NMR provides an evaluation of the carbon and nitrogen status in intact cells, with the ability to identify alterations involving PG and WTA given their unique carbon and nitrogen composition as compared to those of most other cellular constituents (Figure 5B). A whole sample accounting or framework will be valuable in diverse studies involving changes to bacterial cell composition.

ASSOCIATED CONTENT

Supporting Information

The Supporting Information is available free of charge on the ACS Publications website at DOI: 10.1021/acs.biochem.8b00495.

Chemical quantification of inorganic phosphate in cell walls and teichoic acids, quantification of peaks in whole-cell CPMAS spectra, ^{13}C and ^{15}N CPMAS spectra of whole cells under different growth conditions, and ^{15}N CPMAS spectra of whole cells labeled with L-[ε-^{15}N]-lysine and D-[^{15}N]alanine (PDF)

AUTHOR INFORMATION

Corresponding Author

*E-mail: cegelski@stanford.edu. Telephone: 650-725-3527. Fax: 650-723-4817.

ORCID

Lynette Cegelski: 0000-0002-0978-1814

Funding

Research reported in this publication was supported by the National Institute of General Medical Sciences of the National Institutes of Health via Grant R01GM117278.

Notes

The authors declare no competing financial interest.

ACKNOWLEDGMENTS

The authors are grateful to Professor Suzanne Walker for providing *S. aureus* MW2, MW2Δ*dltA*, and MW2Δ*tarO* strains.

REFERENCES

(1) Foster, T. J. (2017) Antibiotic resistance in *Staphylococcus aureus*. Current status and future prospects. *FEMS Microbiol. Rev. 41*, 430−449.

DOI: 10.1021/acs.biochem.8b00495
Biochemistry 2018, 57, 3966−3975

(2) Lovering, A. L., Safadi, S. S., and Strynadka, N. C. (2012) Structural perspective of peptidoglycan biosynthesis and assembly. *Annu. Rev. Biochem. 81*, 451−478.
(3) Egan, A. J., Biboy, J., van't Veer, I., Breukink, E., and Vollmer, W. (2015) Activities and regulation of peptidoglycan synthases. *Philos. Trans. R. Soc., B 370*, 20150031.
(4) Sham, L. T., Butler, E. K., Lebar, M. D., Kahne, D., Bernhardt, T. G., and Ruiz, N. (2014) MurJ is the flippase of lipid-linked precursors for peptidoglycan biogenesis. *Science 345*, 220−222.
(5) Zhao, H., Patel, V., Helmann, J. D., and Dorr, T. (2017) Don't let sleeping dogmas lie: new views of peptidoglycan synthesis and its regulation. *Mol. Microbiol. 106*, 847−860.
(6) Schaefer, K., Matano, L. M., Qiao, Y., Kahne, D., and Walker, S. (2017) *In vitro* reconstitution demonstrates the cell wall ligase activity of LCP proteins. *Nat. Chem. Biol. 13*, 396−401.
(7) Weidenmaier, C., Kokai-Kun, J. F., Kristian, S. A., Chanturiya, T., Kalbacher, H., Gross, M., Nicholson, G., Neumeister, B., Mond, J. J., and Peschel, A. (2004) Role of teichoic acids in *Staphylococcus aureus* nasal colonization, a major risk factor in nosocomial infections. *Nat. Med. 10*, 243−245.
(8) Bertsche, U., Yang, S. J., Kuehner, D., Wanner, S., Mishra, N. N., Roth, T., Nega, M., Schneider, A., Mayer, C., Grau, T., Bayer, A. S., and Weidenmaier, C. (2013) Increased cell wall teichoic acid production and D-alanylation are common phenotypes among daptomycin-resistant methicillin-resistant *Staphylococcus aureus* (MRSA) clinical isolates. *PLoS One 8*, No. e67398, DOI: 10.1371/journal.pone.0067398.
(9) Bayer, A. S., Schneider, T., and Sahl, H. G. (2013) Mechanisms of daptomycin resistance in *Staphylococcus aureus*: role of the cell membrane and cell wall. *Ann. N. Y. Acad. Sci. 1277*, 139−158.
(10) Gautam, S., Kim, T., Lester, E., Deep, D., and Spiegel, D. A. (2016) Wall teichoic acids prevent antibody binding to epitopes within the cell wall of *Staphylococcus aureus*. *ACS Chem. Biol. 11*, 25−30.
(11) Wang, H., Gill, C. J., Lee, S. H., Mann, P., Zuck, P., Meredith, T. C., Murgolo, N., She, X., Kales, S., Liang, L., Liu, J., Wu, J., Santa Maria, J., Su, J., Pan, J., Hailey, J., McGuinness, D., Tan, C. M., Flattery, A., Walker, S., Black, T., and Roemer, T. (2013) Discovery of wall teichoic acid inhibitors as potential anti-MRSA beta-lactam combination agents. *Chem. Biol. 20*, 272−284.
(12) Campbell, J., Singh, A. K., Santa Maria, J. P., Jr., Kim, Y., Brown, S., Swoboda, J. G., Mylonakis, E., Wilkinson, B. J., and Walker, S. (2011) Synthetic lethal compound combinations reveal a fundamental connection between wall teichoic acid and peptidoglycan biosyntheses in *Staphylococcus aureus*. *ACS Chem. Biol. 6*, 106−116.
(13) Lee, S. H., Wang, H., Labroli, M., Koseoglu, S., Zuck, P., Mayhood, T., Gill, C., Mann, P., Sher, X., Ha, S., Yang, S. W., Mandal, M., Yang, C., Liang, L., Tan, Z., Tawa, P., Hou, Y., Kuvelkar, R., DeVito, K., Wen, X., Xiao, J., Batchlett, M., Balibar, C. J., Liu, J., Xiao, J., Murgolo, N., Garlisi, C. G., Sheth, P. R., Flattery, A., Su, J., Tan, C., and Roemer, T. (2016) TarO-specific inhibitors of wall teichoic acid biosynthesis restore beta-lactam efficacy against methicillin-resistant staphylococci. *Sci. Transl. Med. 8*, 329ra32.
(14) Campbell, J., Singh, A. K., Swoboda, J. G., Gilmore, M. S., Wilkinson, B. J., and Walker, S. (2012) An antibiotic that inhibits a late step in wall teichoic acid biosynthesis induces the cell wall stress stimulon in *Staphylococcus aureus*. *Antimicrob. Agents Chemother. 56*, 1810−1820.
(15) Brown, S., Santa Maria, J. P., Jr., and Walker, S. (2013) Wall teichoic acids of gram-positive bacteria. *Annu. Rev. Microbiol. 67*, 313−336.
(16) Brown, S., Xia, G., Luhachack, L. G., Campbell, J., Meredith, T. C., Chen, C., Winstel, V., Gekeler, C., Irazoqui, J. E., Peschel, A., and Walker, S. (2012) Methicillin resistance in *Staphylococcus aureus* requires glycosylated wall teichoic acids. *Proc. Natl. Acad. Sci. U. S. A. 109*, 18909−18914.
(17) Schirner, K., Stone, L. K., and Walker, S. (2011) ABC transporters required for export of wall teichoic acids do not discriminate between different main chain polymers. *ACS Chem. Biol. 6*, 407−412.
(18) Schaefer, K., Owens, T. W., Kahne, D., and Walker, S. (2018) Substrate Preferences Establish the Order of Cell Wall Assembly in *Staphylococcus aureus*. *J. Am. Chem. Soc. 140*, 2442−2445.
(19) Reichmann, N. T., Cassona, C. P., and Grundling, A. (2013) Revised mechanism of D-alanine incorporation into cell wall polymers in Gram-positive bacteria. *Microbiology 159*, 1868−1877.
(20) Schneewind, O., and Missiakas, D. (2014) Lipoteichoic acids, phosphate-containing polymers in the envelope of gram-positive bacteria. *J. Bacteriol. 196*, 1133−1142.
(21) Santa Maria, J. P., Jr., Sadaka, A., Moussa, S. H., Brown, S., Zhang, Y. J., Rubin, E. J., Gilmore, M. S., and Walker, S. (2014) Compound-gene interaction mapping reveals distinct roles for *Staphylococcus aureus* teichoic acids. *Proc. Natl. Acad. Sci. U. S. A. 111*, 12510−12515.
(22) Kho, K., and Meredith, T. C. (2018) Salt-Induced Stress Stimulates a Lipoteichoic Acid-Specific Three Component Glycosylation System in *Staphylococcus aureus*. *J. Bacteriol. 200*, e00017-18.
(23) Kahan, F. M., Kahan, J. S., Cassidy, P. J., and Kropp, H. (1974) The mechanism of action of fosfomycin (phosphonomycin),. *Ann. N. Y. Acad. Sci. 235*, 364−386.
(24) Kahne, D., Leimkuhler, C., Lu, W., and Walsh, C. (2005) Glycopeptide and lipoglycopeptide antibiotics. *Chem. Rev. 105*, 425−448.
(25) Cho, H., Uehara, T., and Bernhardt, T. G. (2014) Beta-lactam antibiotics induce a lethal malfunctioning of the bacterial cell wall synthesis machinery. *Cell 159*, 1300−1311.
(26) Ling, L. L., Schneider, T., Peoples, A. J., Spoering, A. L., Engels, I., Conlon, B. P., Mueller, A., Schaberle, T. F., Hughes, D. E., Epstein, S., Jones, M., Lazarides, L., Steadman, V. A., Cohen, D. R., Felix, C. R., Fetterman, K. A., Millett, W. P., Nitti, A. G., Zullo, A. M., Chen, C., and Lewis, K. (2015) A new antibiotic kills pathogens without detectable resistance,. *Nature 517*, 455−459.
(27) Fiers, W. D., Craighead, M., and Singh, I. (2017) Teixobactin and Its Analogues: A New Hope in Antibiotic Discovery,. *ACS Infect. Dis. 3*, 688−690.
(28) Lee, W., Schaefer, K., Qiao, Y., Srisuknimit, V., Steinmetz, H., Muller, R., Kahne, D., and Walker, S. (2016) The Mechanism of Action of Lysobactin,. *J. Am. Chem. Soc. 138*, 100−103.
(29) Qiao, Y., Srisuknimit, V., Rubino, F., Schaefer, K., Ruiz, N., Walker, S., and Kahne, D. (2017) Lipid II overproduction allows direct assay of transpeptidase inhibition by beta-lactams. *Nat. Chem. Biol. 13*, 793−798.
(30) Glauner, B. (1988) Separation and quantification of muropeptides with high-performance liquid chromatography. *Anal. Biochem. 172*, 451−464.
(31) Zhou, X., and Cegelski, L. (2012) Nutrient-dependent structural changes in *S. aureus* peptidoglycan revealed by solid-state NMR spectroscopy. *Biochemistry 51*, 8143−8153.
(32) Kuru, E., Hughes, H. V., Brown, P. J., Hall, E., Tekkam, S., Cava, F., de Pedro, M. A., Brun, Y. V., and VanNieuwenhze, M. S. (2012) In Situ probing of newly synthesized peptidoglycan in live bacteria with fluorescent D-amino acids. *Angew. Chem., Int. Ed. 51*, 12519−12523.
(33) Sugimoto, A., Maeda, A., Itto, K., and Arimoto, H. (2017) Deciphering the mode of action of cell wall-inhibiting antibiotics using metabolic labeling of growing peptidoglycan in *Streptococcus pyogenes*. *Sci. Rep. 7*, 1129.
(34) Cegelski, L., Kim, S. J., Hing, A. W., Studelska, D. R., O'Connor, R. D., Mehta, A. K., and Schaefer, J. (2002) Rotational-echo double resonance characterization of the effects of vancomycin on cell wall synthesis in *Staphylococcus aureus*. *Biochemistry 41*, 13053−13058.
(35) Cegelski, L., Steuber, D., Mehta, A. K., Kulp, D. W., Axelsen, P. H., and Schaefer, J. (2006) Conformational and quantitative characterization of oritavancin-peptidoglycan complexes in whole cells of *Staphylococcus aureus* by in vivo 13C and 15N labeling. *J. Mol. Biol. 357*, 1253−1262.
(36) Kim, S. J., Chang, J., and Singh, M. (2015) Peptidoglycan architecture of Gram-positive bacteria by solid-state NMR. *Biochim. Biophys. Acta, Biomembr. 1848*, 350−362.

DOI: 10.1021/acs.biochem.8b00495
Biochemistry 2018, 57, 3966−3975

(37) Kim, S. J., Singh, M., Sharif, S., and Schaefer, J. (2014) Cross-link formation and peptidoglycan lattice assembly in the FemA mutant of *Staphylococcus aureus*. *Biochemistry 53*, 1420−1427.
(38) Yang, H., Singh, M., Kim, S. J., and Schaefer, J. (2017) Characterization of the tertiary structure of the peptidoglycan of *Enterococcus faecalis*. *Biochim. Biophys. Acta, Biomembr. 1859*, 2171−2180.
(39) Bui, N. K., Eberhardt, A., Vollmer, D., Kern, T., Bougault, C., Tomasz, A., Simorre, J. P., and Vollmer, W. (2012) Isolation and analysis of cell wall components from *Streptococcus pneumoniae*. *Anal. Biochem. 421*, 657−666.
(40) Kern, T., Giffard, M., Hediger, S., Amoroso, A., Giustini, C., Bui, N. K., Joris, B., Bougault, C., Vollmer, W., and Simorre, J. P. (2010) Dynamics characterization of fully hydrated bacterial cell walls by solid-state NMR: evidence for cooperative binding of metal ions. *J. Am. Chem. Soc. 132*, 10911−10919.
(41) Berejnaia, O., Wang, H., Labroli, M., Yang, C., Gill, C., Xiao, J., Hesk, D., DeJesus, R., Su, J., Tan, C. M., Sheth, P. R., Kavana, M., and McLaren, D. G. (2017) Quantitation of wall teichoic acid in *Staphylococcus aureus* by direct measurement of monomeric units using LC-MS/MS. *Anal. Biochem. 518*, 9−15.
(42) Nygaard, R., Romaniuk, J. A., Rice, D. M., and Cegelski, L. (2015) Spectral snapshots of bacterial cell-wall composition and the influence of antibiotics by whole-cell NMR. *Biophys. J. 108*, 1380−1389.
(43) Rice, D. M., Romaniuk, J. A., and Cegelski, L. (2015) Frequency-selective REDOR and spin-diffusion relays in uniformly labeled whole cells. *Solid State Nucl. Magn. Reson. 72*, 132−139.
(44) Lusk, G., and Gullion, T. (2018) Description of an rf field-strength controller for solid-state NMR experiments. *Solid State Nucl. Magn. Reson. 91*, 9−14.
(45) Schaefer, J., and Stejskal, E. O. (1976) Carbon-13 Nuclear Magnetic Resonance of Polymers Spinning at the Magic Angle. *J. Am. Chem. Soc. 98*, 1031−1032.
(46) Chen, P., Toribara, T. t., and Warner, H. (1956) Micro-determination of phosphorus. *Anal. Chem. 28*, 1756−1758.
(47) Ames, B. N., and Dubin, D. T. (1960) The role of polyamines in the neutralization of bacteriophage deoxyribonucleic acid. *J. Biol. Chem. 235*, 769−775.
(48) Swoboda, J. G., Campbell, J., Meredith, T. C., and Walker, S. (2010) Wall teichoic acid function, biosynthesis, and inhibition. *ChemBioChem 11*, 35−45.
(49) Bera, A., Biswas, R., Herbert, S., Kulauzovic, E., Weidenmaier, C., Peschel, A., and Gotz, F. (2007) Influence of wall teichoic acid on lysozyme resistance in *Staphylococcus aureus*. *J. Bacteriol. 189*, 280−283.
(50) Bera, A., Herbert, S., Jakob, A., Vollmer, W., and Gotz, F. (2005) Why are pathogenic staphylococci so lysozyme resistant? The peptidoglycan O-acetyltransferase OatA is the major determinant for lysozyme resistance of *Staphylococcus aureus*. *Mol. Microbiol. 55*, 778−787.
(51) Bertsche, U., Weidenmaier, C., Kuehner, D., Yang, S. J., Baur, S., Wanner, S., Francois, P., Schrenzel, J., Yeaman, M. R., and Bayer, A. S. (2011) Correlation of daptomycin resistance in a clinical *Staphylococcus aureus* strain with increased cell wall teichoic acid production and D-alanylation. *Antimicrob. Agents Chemother. 55*, 3922−3928.
(52) Nygaard, R., Romaniuk, J. A. H., Rice, D. M., and Cegelski, L. (2017) Whole Ribosome NMR: Dipolar Couplings and Contributions to Whole Cells. *J. Phys. Chem. B 121*, 9331−9335.
(53) Pasquina, L., Santa Maria, J. P., Jr., McKay Wood, B., Moussa, S. H., Matano, L. M., Santiago, M., Martin, S. E., Lee, W., Meredith, T. C., and Walker, S. (2016) A synthetic lethal approach for compound and target identification in *Staphylococcus aureus*,. *Nat. Chem. Biol. 12*, 40−45.
(54) Romaniuk, J. A., and Cegelski, L. (2015) Bacterial cell wall composition and the influence of antibiotics by cell-wall and whole-cell NMR. *Philos. Trans. R. Soc., B 370*, 20150024.
(55) McDowell, L. M., Schmidt, A., Cohen, E. R., Studelska, D. R., and Schaefer, J. (1996) Structural constraints on the ternary complex of 5-enolpyruvylshikimate-3-phosphate synthase from rotational-echo double-resonance NMR. *J. Mol. Biol. 256*, 160−171.
(56) Hakulinen, J. K., Hering, J., Branden, G., Chen, H., Snijder, A., Ek, M., and Johansson, P. (2017) MraY-antibiotic complex reveals details of tunicamycin mode of action. *Nat. Chem. Biol. 13*, 265−267.
(57) Kim, S. J., Cegelski, L., Preobrazhenskaya, M., and Schaefer, J. (2006) Structures of *Staphylococcus aureus* cell-wall complexes with vancomycin, eremomycin, and chloroeremomycin derivatives by 13C{19F} and 15N{19F} rotational-echo double resonance. *Biochemistry 45*, 5235−5250.

DOI: 10.1021/acs.biochem.8b00495
Biochemistry 2018, 57, 3966−3975